Maternal Control of Development at the Midblastula Transition and beyond : Mutants from the Zebrafish II

Wagner, Daniel S.; Dosch, Roland; Mintzer, Keith A.; Wiemelt, Anthony P.; Mullins, Mary C.

Developmental Cell, Vol. 6, 781–790, June, 2004, Copyright ©2004 by Cell Press

Maternal Control of Development at the Midblastula Transition and beyond: Mutants from the Zebrafish II

Daniel S. Wagner,[1,2] Roland Dosch,[1,3] Keith A. Mintzer, Anthony P. Wiemelt, and Mary C. Mullins*
Department of Cell & Developmental Biology
University of Pennsylvania Medical School
1211 BRBII/III
421 Curie Boulevard
Philadelphia, Pennsylvania 19104

Summary

Many maternal factors in the oocyte persist in the embryo. They are required to initiate zygotic transcription but also function beyond this stage, where they interact with zygotic gene products during embryonic development. In a four-generation screen in the zebrafish, we identified 47 maternal-effect and five paternal-effect mutants that manifest their phenotypes at the time of, or after, zygotic genome activation. We propagated a subset of 13 mutations that cause developmental arrest at the midblastula transition, defects in cell viability, embryonic morphogenesis, and establishment of the embryonic body plan. This diverse group of mutants, many not previously observed in vertebrates, demonstrates a substantial maternal contribution to the "zygotic" period of embryogenesis and a surprising degree of paternal control. These mutants provide powerful tools to dissect the maternal and paternal control of vertebrate embryogenesis.

Introduction

The degree to which the maternal genome controls embryonic development in different organisms depends in part on the stage at which zygotic transcription initiates (reviewed in Andeol, 1994). However, maternal influence on embryogenesis also persists beyond the onset of zygotic transcription at the midblastula transition (MBT). Maternal-effect mutants with morphological defects first evident following the MBT have been identified in flies, fish, and amphibians (Gans et al., 1975; Raftery et al., 1995; Schupbach and Wieschaus, 1989; Sekelsky et al., 1995; Steward et al., 1984; Terracol and Lengyel, 1994; Zalokar et al., 1975). In the mouse, zygotic transcription begins at the 2-cell stage (Bolton et al., 1984; Flach et al., 1982). However, a large number of maternal mRNAs persist beyond the 2-cell stage (Bachvarova and De Leon, 1980; Bachvarova and Moy, 1985), some of which are known to function after the onset of zygotic transcription. For example, Om/DDK, *mater*, Hsf1, and Zar1 maternal genes are required for progression past the 2- or 4-cell stages (Christians et al., 2000; Renard et al., 1994; Tong et al., 2000; Wu et al., 2003), and elimination of Formin-2 (Leader et al., 2002) or two DNA methyltransferases involved in imprinting (Bourc'his et al., 2001; Howell et al., 2001) causes late maternal-effect lethality.

The nature of this persisting maternal influence does not require that the maternal factor function after the MBT. Some maternal factors function before the MBT, although their phenotypic consequences are not visible morphologically until after it. Other maternal factors persist beyond the MBT, when they are required for specific post-MBT processes and function together with zygotic gene products (Gritsman et al., 1999; Miller-Bertoglio et al., 1999; Mintzer et al., 2001; Raftery et al., 1995; Sekelsky et al., 1995; Steward et al., 1984; Terracol and Lengyel, 1994).

To study such processes, we conducted a four-generation maternal-effect mutant screen in the zebrafish (described in Dosch et al., 2004, this issue). We screened 600 mutagenized genomes and identified 68 maternal-effect mutants. In addition, we recovered 17 adult morphologically visible mutants and five paternal-effect mutants, demonstrating the utility of our screen to identify multiple classes of adult mutant phenotypes. In this report, we describe some of these mutants, as well as 47 "late" maternal-effect mutants, which manifest their phenotypes at or following the MBT. Some of these mutants represent genes acting during the zygotic period of embryogenesis, bridging the transition from maternal to zygotic control of development. These mutants bring a powerful molecular-genetic tool to vertebrates for elucidating the molecular mechanisms of maternal and paternal control of vertebrate development.

Results and Discussion

The majority of maternal-effect mutants (47 of 68) identified in our screen manifested their phenotypes at or following the MBT, referred to as the "late" phenotypes. The early mutants are described in the accompanying article (Dosch et al., 2004). We placed the late mutants into five phenotypic classes: developmental arrest, epiboly, pattern formation, body plan, and general cell viability (Table 1). All of these mutants are strict, recessive maternal-effect mutants. That is, the embryonic phenotypes depend solely on the genotype of the mother, displaying no paternal rescue or recessive maternal-zygotic requirement. All analysis described below was performed on embryos from mutant females crossed to wild-type males.

Developmental Arrest Mutants

During blastula cleavages, the ratio of nuclear to cytoplasmic volume increases with each cell division. Embryos undergo the MBT when this ratio reaches a critical threshold. In zebrafish, this occurs at the 512-cell stage (Kane and Kimmel, 1993). In *Xenopus* and zebrafish, the MBT is characterized by a loss of cell division synchrony, an increase in cell motility, and the onset of wholesale

*Correspondence: mullins@mail.med.upenn.edu
[1]These authors contributed equally to this work.
[2]Present address: Department of Biochemistry and Cell Biology, Rice University, MS-140, PO Box 1892, Houston, TX 77251.
[3]Present address: Departement de Zoologie et biologie animal, Universite de Geneve, Sciences III, 30 quai Ernest-Ansermet, CH-1211 Geneve, Switzerland.

Table 1. Maternal- and Paternal-Effect Mutants with Phenotypes at and beyond the MBT

Class	Number of Mutants Identified	Genes/Alleles
Developmental arrest	3	*screeching halt*^{p18ad}
Epiboly defect	4	*betty boop*^{p58cd}, *poky*^{p20ad}, *slow*^{p3er}, *bedazzled*^{p21re}
Pattern formation	2	*brom bones*^{p50ada}, *pug*^{p37mfb}
Body plan	2	*blistered*^{p12cdb}, *pollywog*^{p35mfa}
Cell viability	36	
Paternal-effect	5	*cronus*^{p32mf}, *p5bn*, *p24ad*, *p95re*

"Number of mutants identified" indicates total number of mutants found in the class. "Genes/Alleles" lists only the lines that were propagated. Gene names were given to alleles that have either been mapped to a chromosomal position or excluded from linkage to other mutations in the same class. An allele designation without a gene name indicates that the mutation has not been excluded as allelic to another gene in the class.

zygotic transcription (Kane and Kimmel, 1993; Newport and Kirschner, 1982a, 1982b). Three mutants identified in our screen developed normally during early blastula stages, but then arrested around the MBT. Morphologically, these mutants remain at a midblastula stage, while wild-type controls continue through gastrula stages (Figures 1A and 1B).

We investigated cell division and the initiation of zygotic gene expression in the mutant *screeching halt* (*srh*), two cellular behaviors that change at the MBT. We observed by time-lapse video microscopy fewer dividing cells at the surface of mutant embryos following the MBT than in age-matched wild-type embryos (data not shown and Supplemental Data [http://www.developmentalcell.com/cgi/content/full/6/6/781/DC1]). At 4 hr post fertilization (hpf, ~1 hr post-MBT), mutant cells exhibited phosphohistone-H3 staining, which marks condensed chromatin in metaphase and early anaphase cells (Figures 1C and 1D). However, the mutant cells remained large and the number of nuclei failed to increase to the level of controls. Additionally, aberrant chromatin morphology appeared at the MBT. Approximately half of the nuclei of 512-cell stage mutant embryos displayed strings of DAPI-positive material connecting pairs of nuclei, suggesting a defect in chromosome segregation. This nuclear phenotype progressively worsens. At sphere stage, mutant embryos contain fragmented chromatin in addition to the strings of nuclear material (Figures 1C and 1D). Thus cell division is disrupted in mutant embryos, leading to a breakdown of nuclear integrity while the cells are attempting to divide.

To investigate the onset of zygotic gene expression in *screeching halt* embryos, we analyzed several genes that initiate expression between the MBT and the onset of gastrulation. Expression of *bmp2b*, *eve1*, *no tail* (*ntl*), and *spadetail* was initiated in mutant embryos, but it lacked its normal restricted expression domain. The expression of *ntl* consisted of scattered positive cells around the margin and a central clearing (Figures 1E and 1F), whereas the others exhibited positive cells throughout the blastoderm (data not shown). The genes *dharma*, *tbx6*, and *sonic hedgehog* (*shh*) failed to be expressed (Figures 1G and 1H and data not shown). Thus *screeching halt* mutant embryos display a defect in the coordinated initiation of zygotic gene expression after the MBT.

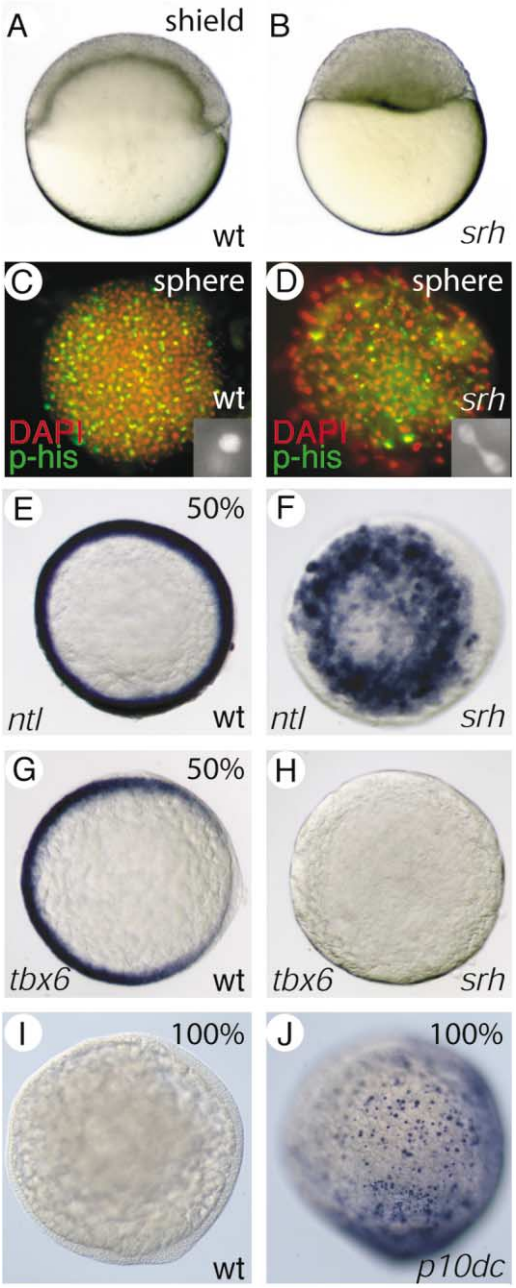

Figure 1. Developmental Arrest and Cell Viability Mutants

A wild-type embryo at shield stage (A) and an age-matched *srh* embryo (B). Wild-type (C) and *srh* (D) embryos at sphere stage stained for nuclei (red and insets) and anti-phosphohistone (green). *ntl* expression in wild-type (E) and *srh* (F) embryos. The expression of *tbx6* in wild-type (G) was not observed in age-matched *srh* embryos (H). Whole-mount terminal transferase assay on wild-type (I) and *p10dc* embryos (J). (A, B, I, and J) Lateral view, animal pole up, (C–H) animal view, (A, G, I, and J) dorsal to the right. (E, G, I, and J) Percent epiboly is shown.

Zygotic transcription is not required for continued cell division in zebrafish, whereas it is required for the initiation of morphogenetic movements (Kane et al., 1996). Hence, the lack of morphogenetic movements in *screeching halt* mutants may be secondary to the loss of zygotic gene expression, but the cell division defect is not.

Two maternal-effect mutants in *Drosophila* that affect the MBT, *grapes* and *mei-41*, display abnormal nuclear morphology and a defect in zygotic gene expression after the MBT (Sibon et al., 1999, 1997), resembling that observed in *screeching halt* mutants. The *grapes* and *mei-41* genes are homologs of the Chk1 and ATR kinases, respectively, which are components of a DNA replication checkpoint control. In both *Drosophila* and *Xenopus*, they are hypothesized to slow the cell cycle at the MBT in response to the titration of an unknown maternal component required for DNA replication (Fogarty et al., 1997; Shimuta et al., 2002; Sibon et al., 1999, 1997). Based on the similarity of mutant phenotypes, *screeching halt* may be a component of this process involved in executing the MBT in zebrafish.

Pleiotropic Cell Viability Mutants

The largest mutant class identified in our screen, representing about half of all the mutants (36 of 68), showed a pleiotropic degeneration phenotype, which typically appeared as widespread cell death. We confirmed that extensive apoptosis occurred in two of the mutants using a terminal transferase assay (Figures 1I and 1J and data not shown). These mutants resemble a large class of pleiotropic zygotic "necrosis" mutants (Abdelilah et al., 1996; Furutani-Seiki et al., 1996; Mullins et al., 1994), but cell death initiated much earlier in the maternal-effect mutants, some becoming evident as soon as the embryo is competent to execute an apoptotic program at 60% epiboly (Ikegami et al., 1999). We expected to identify such a class of mutants and predict that the majority are mutations in general cellular machinery or housekeeping genes, as recently found for several zygotic necrosis mutants (Golling et al., 2002). These maternal-effect mutants probably accrue cellular damage during early development due to the loss of a required maternal component, leading to the execution of the apoptotic program as soon as the embryo is competent to do so.

Epiboly Mutants

Epiboly in zebrafish involves the coordinated, dynamic movement of three distinct cell layers that spread over the surface of the yolk from the animal pole to the vegetal pole (Figures 2A–2D, Solnica-Krezel and Driever, 1994; Warga and Kimmel, 1990). The enveloping layer (EVL) is an external epithelium. The deep layer (DEL) is the internal blastula cells that form the embryo proper. Underlying the DEL is the yolk syncytial layer (YSL), a nuclear syncytium postulated to be a driving force in epiboly (Betchaku and Trinkaus, 1978; Strahle and Jesuthasan, 1993). Few morphogenesis mutants were recovered from zygotic screens in zebrafish, likely due to a large maternal contribution to the control of morphogenesis in the zebrafish, as our results indicate here (see also *pollywog* below).

The mutant *betty boop* (*bbp*) was indistinguishable from wild-type during cleavage and early epiboly stages. However, when gastrulation initiates at 50% epiboly, the margin of the gastrula constricts around its circumference and the yolk cell lyses (Figures 2E and 2F). We observed no change in expression of the mesodermal marker *ntl* or the dorsally expressed gene *chordino* (data not shown). Therefore, misspecification of mesoderm or dorsal identity is unlikely to cause the aberrant morphogenetic movements. The time window of marginal constriction of the *betty boop* mutant coincides with the movement of the YSL margin ahead of the DEL (Figures 2C and 2D). This transition in the relationship of these layers may represent a change in the primary mechanism of force generation driving epiboly. The *betty boop* mutant fails to make this transition, possibly due to its inability to withstand new forces that arise at this transition or a defect in a force generating process required at this time.

Two mutants, *poky* (*pky*) and *slow* (*sow*), are delayed in epiboly, whereas other processes occur on a normal schedule. Time-lapse video microscopy of *poky* embryos indicates that the latter half of epiboly is slowed more significantly than the first half (Figure 2G; Supplemental Data). All three cell layers in *poky* mutants are defective in epiboly movements, as revealed in time-lapse microscopy studies (Figures 2L–2N and Supplemental Data). Frequently, the yolk cell of *poky* mutants lyses before epiboly is completed (data not shown).

In *slow* mutant embryos, the DEL is more strongly affected than the other layers, as seen in time-lapse video microscopy of live embryos (Supplemental Data). This indicates distinct molecular controls of DEL versus YSL and EVL cell movements. A similar conclusion arose in analysis of the maternal-zygotic epiboly mutant *half-baked*, which arrests in movement of the DEL, but not the EVL and YSL (Kane et al., 1996). Frequently, the DEL of *slow* mutant embryos fails to complete epiboly, while the EVL and YSL do, resulting in defects associated with defective blastopore closure. Embryos that survive to 1 day post fertilization (dpf) display a range of phenotypes from mild kinks in the notochord (data not shown) to a severe "open back" phenotype (Figures 2Y and 2Z), caused by splitting of the paraxial and neural tissue around a dorsal protruding yolk.

Although epiboly is delayed in *poky* and *slow* mutants, differentiation of the embryo is not. Somitogenesis, which begins following epiboly, initiated at approximately the same time point in mutants as in age-matched wild-type controls, although the mutants had not completed epiboly (see Supplemental Data). Additionally, expression of *pax2.1* in the mid-hindbrain boundary initiated concurrently in *poky* and *slow* embryos as in age-matched controls, although mutant embryos had not reached 90% epiboly, the stage at which *pax2.1* is normally first expressed (Krauss et al., 1991) (Figures 2H and 2I and data not shown).

We determined the chromosomal positions of the *poky* and *slow* mutations, using a mapping cross integrated within our screen strategy (described in Dosch et al., 2004, this issue). As expected from the differences in their mutant phenotypes, these mutations alter distinct genes. The *poky* mutation lies in a 20 cm interval

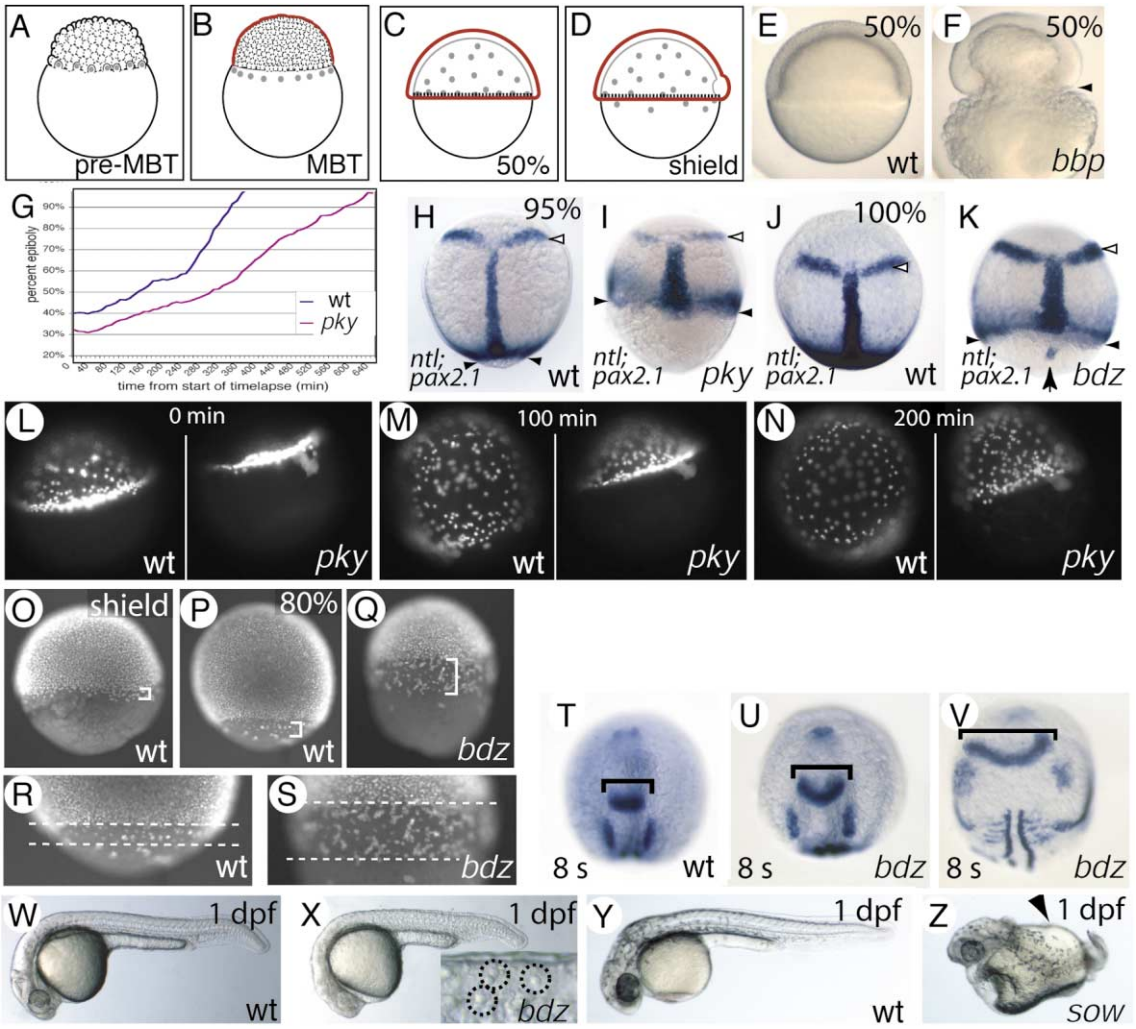

Figure 2. Epiboly Mutants

(A–D) Schematic of zebrafish epiboly. (A) The YSN originate from marginal cells that maintain cytoplasmic bridges with the yolk (gray nuclei). (B) At MBT, the marginal cell membranes regress and their nuclei form a syncytium atop the yolk, the yolk syncytial layer (YSL, gray nuclei), which extends beyond the margin of the blastoderm. The external enveloping layer (EVL, red cells) forms an epithelium that surrounds the internal deep layer (DEL, white cells), which forms the embryo proper. (C) At 50% epiboly, the blastoderm covers 50% of the yolk and the EVL (red line) and DEL (dashed line) margins have overtaken the YSL margin. (D) The YSL continues to advance toward the vegetal pole while the DEL and EVL pause during the initiation of gastrulation at shield stage.

(E) Wild-type embryo at 50% epiboly. (F) Age-matched *bbp* mutant. The blastoderm is constricted at the margin (arrowhead) and the yolk cell has lysed. (G) A graph of the progression through epiboly averaged for two wild-type (blue line) and two *pky* mutant (red line) embryos. Expression of *ntl* (black arrowheads) and *pax2.1* (white arrowhead) in a 95% epiboly wild-type (H) and age-matched *pky* mutant (I) embryo. Expression of *ntl* (black arrowheads) and *pax2.1* (white arrowhead) in a 100% epiboly wild-type (J) and an age-matched *bdz* mutant embryo (K) (arrow, *ntl* positive forerunner cells).

(L–N) Epiboly progression of sytox green labeled yolk syncytial nuclei (YSN) in wild-type and age-matched *pky* mutants viewed under fluorescent illumination. Animal pole is oriented ~20° counterclockwise from the top; series begins at approximately 50% epiboly in wild-type.

DAPI-stained embryos reveal a wide separation of the EVL and YSL margins from the DEL margin in *bdz* mutants (O–S). Wild-type embryos at shield stage (O) and 80% epiboly (P and R) display a small separation of the EVL and YSL margins from the DEL margin (bracket and dashed lines in [R]). Age-matched *bdz* mutant embryo to 80% epiboly wild-type embryo displays a wide separation of the EVL and DEL margins (bracket in [Q] and dashed lines in [S]).

(T–V) *bdz* mutant embryos display a variably broadened neural plate at the ~8-somite stage, as indicated by the width of *pax2.1* expression in the MHB and otic placodes (brackets). One dpf wild-type (W) and *bdz* mutant (X) embryo, which displays rounded cells throughout the embryo. Inset (X), higher magnification of trunk with three rounded cells indicated (dashed circles). An age-matched wild-type (Y) and strongly affected *sow* mutant embryo (Z) at 1 dpf. The *sow* mutant displays an "open back" phenotype (arrowhead). (E, F, and L–S) lateral view, animal pole up. (H–K, T–V) Dorsal view, anterior up. (W–Z) Lateral view, rostral to the left.

between SSLP markers z6104 and z9868 on chromosome 13, whereas *slow* lies between z8216 and z13880 on chromosome 7 (data not shown). Furthermore, the *betty boop* mutation is not linked to either of these chromosomal regions (B. Holloway and M.C.M., unpublished data). Thus, our mutants allowed us to dissect the pro-

cess of epiboly into distinct steps controlled by three key genes that drive and coordinate this morphogenetic process: *betty boop* is required for progression past the 50% epiboly stage, *poky* is required for movement of all three cell layers in epiboly, whereas *slow* function predominates in the deep layer.

Unlike the other epiboly mutants, the *bedazzled* (*bdz*) mutant exhibits defects in addition to abnormal epiboly movements. *bedazzled* mutant embryos are delayed in epiboly, displaying a wide separation of the EVL and DEL margins during mid-epiboly stages, indicating a more severe effect on the DEL than the EVL (Figures 2O–2S). Despite the delay in epiboly, differentiation occurred on schedule, and as with *poky* and *slow* mutants, *pax2.1* expression was initiated before *bedazzled* embryos reached 90% epiboly (Figures 2J and 2K). During somitogenesis, a medial-lateral broadened neural keel is evident, suggesting a defect in dorsal convergence as well (Figures 2T–2V). Unlike the other epiboly mutants, loose cells within the blastoderm slough off the EVL during epiboly (Supplemental Data), possibly reflecting a defect in cell adhesion. At 1 dpf, embryos were delayed relative to age-matched controls and large cells were observed superficially on the embryo that persisted for several days (Figures 2W and 2X). A variable fraction also displayed phenotypes associated with defective blastopore closure, whereas others failed to survive to 1 dpf (data not shown). We postulate that the *bedazzled* gene acts in a cellular process associated with both epiboly and dorsal convergence.

Pattern Formation Mutants

Four mutants were identified with specific defects in the embryonic body plan, two of which display clear alterations in pattern formation. The mutant *brom bones* (*brb*) displays a variably penetrant ventralized phenotype (Figures 3A–3C). Mildly affected embryos exhibit a small head and eyes (data not shown). Intermediate strength embryos lack head and notochord (Figure 3B). The most strongly affected embryos display no dorsally derived structures and are radially ventralized (Figure 3C). The small fraction of unaffected embryos (Figure 3A) survives to adulthood. The specification of dorsal identity occurs through establishment of the dorsal Spemann organizer and is known to require maternal-acting factors in a Wnt/β-catenin pathway in frogs and zebrafish (reviewed in Hibi et al., 2002; Sokol, 1999). A similar ventralized phenotype is also observed in the zebrafish maternal-effect mutant *ichabod*, which may be a novel component of a Wnt/β-catenin pathway (Kelly et al., 2000). However, the *brom bones* mutation is not linked to the *ichabod* mutation (Kelly et al., 2000; W. Mei and M.C.M., unpublished data), demonstrating that distinct maternal genes are mutated. The *brom bones* gene is likely to act in the establishment or function of the dorsal organizer.

Embryos from *pug* mutant mothers display a fully penetrant, near-complete loss of the tail. Strongly affected mutants also exhibit defects in the midbrain and cerebellum and lack the pectoral fins (Figures 3D–3F and data not shown). Midbrain regionalization arises from inductive signals from the isthmic organizer, a center in the midbrain-hindbrain boundary (MHB) region. To investigate if the isthmic organizer is affected in this mutant, we examined the expression of several genes that mediate its function. We found normal expression of *en1*, *pax2.1*, and *fgf8* in the MHB at the 10-somite stage,

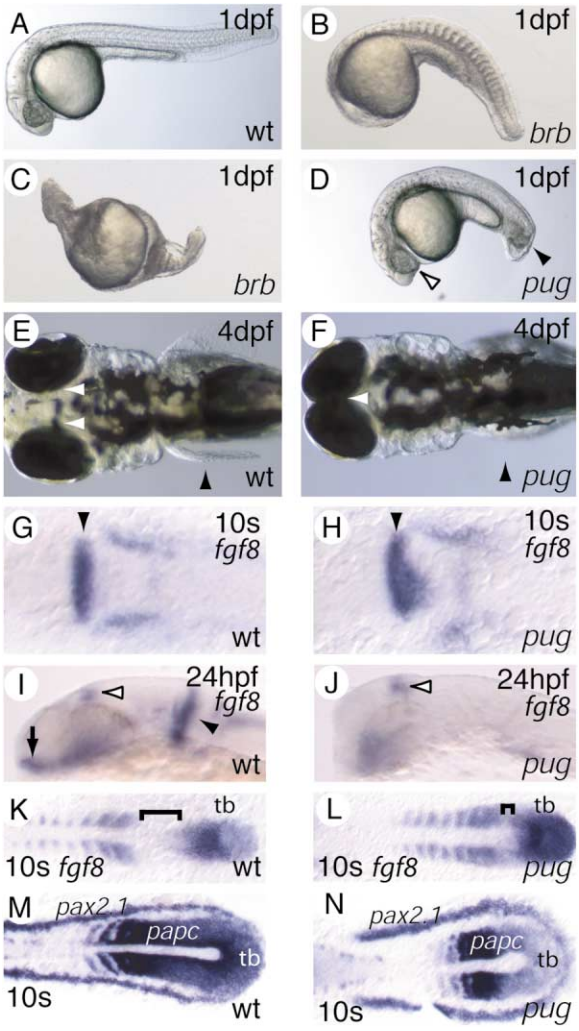

Figure 3. Pattern Formation Mutants

The ventralized mutant *brb* displays a range of phenotypes at 1 dpf from wild-type (A), to partial loss of dorsal structures (B) and radially ventralized (C). (D) At 1 dpf, mutant *pug* embryos display a short tail with a gray mass of dead cells at the tip (black arrowhead), anteriorly displaced eyes (white arrowhead in [D]). (E) At 4 dpf, wild-type embryos exhibit developed pectoral fins and widely spaced eyes, whereas strongly affected *pug* mutants lack pectoral fins (arrowhead) and display narrow-set eyes (white arrowhead) (F). Expression of *fgf8* in the MHB (arrowhead) in wild-type (G) and *pug* (H) embryos at the 10-somite stage. MHB (black arrowhead) and ventral facial ectoderm (arrow) expression domains of fgf8 are present in 24 hpf wild-type ([I], black arrowhead), but not in *pug* mutant embryos (J), whereas another cranial expression domain is present (white arrowhead). At the 10-somite stage, the posterior expression pattern of *fgf8* in wild-type (K) is altered in *pug* mutants (L) with a reduction in the *fgf8* negative domain (bracket) and an increase in tail bud (tb) expression. (M and N) Similarly, *papc* expression in the paraxial mesoderm is shortened in mutants at the 10-somite stage compared to wild-type. Tail bud (tb) *papc* expression is also reduced in mutants.

(A–D, I, and J) Lateral view, rostral to the left. (E–H, K–N) Dorsal view, rostral to the left.

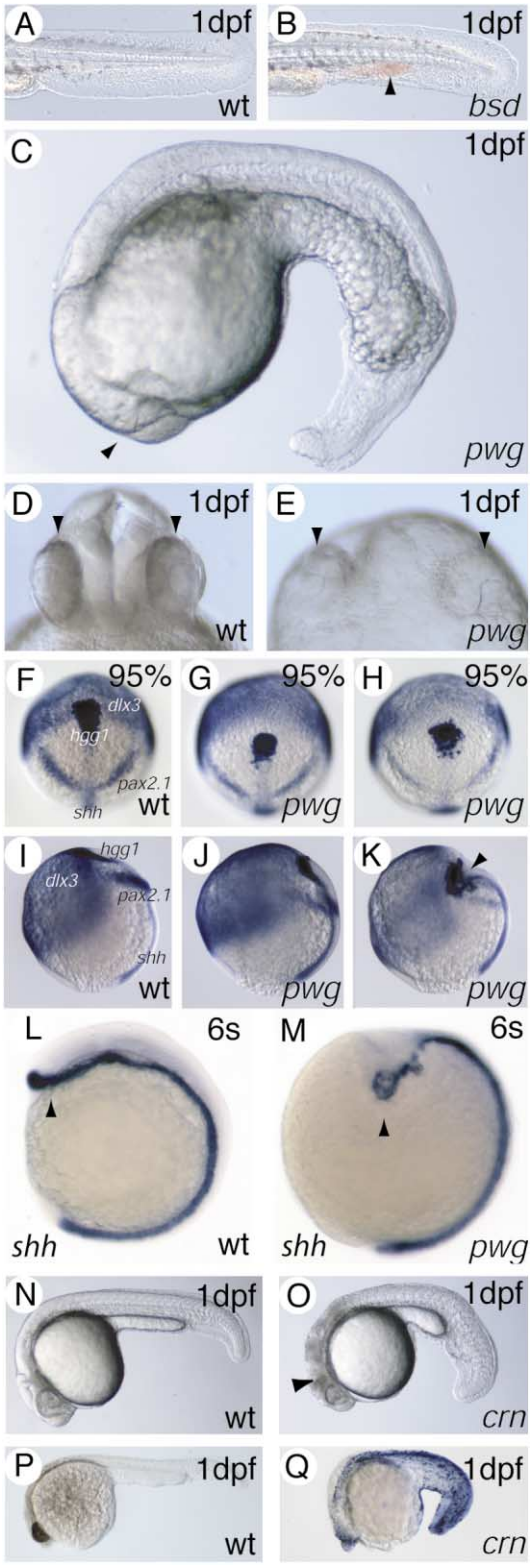

Figure 4. Body Plan Mutants

At 1 dpf, *bsd* embryos display a variably penetrant edema in the ventral tail vein, which accumulates blood (arrowhead, [B]), compared to unaffected siblings (A). (C) At 1 dpf, *pwg* embryos display a flattened head (arrowhead) and fail to extend the tail. Frontal views (dorsal to the top) of wild-type (D) and *pwg* embryos (E). The eyes in the mutant embryo are widely spaced and embedded in the yolk (arrowheads).

indicating that the isthmic organizer forms in *pug* mutants (Figures 3G and 3H and data not shown). However, by 24 hpf, expression of these genes was greatly reduced or absent (Figures 3I and 3J and data not shown). Thus the *pug* gene is not necessary for induction of the isthmic organizer, but is required for its maintenance. In addition to the loss of *fgf8* in the MHB, the anteriormost expression of *fgf8* is absent at 24 hpf (Figures 3I and 3J), reflecting the loss of anterior tissues observed in live embryos (Figures 3D–3F).

The posterior mesoderm is also altered in *pug* mutants. *fgf8* is normally expressed in somites as they form, as well as in a caudal presomitic mesoderm domain and within the tail bud (Figure 3K). Between the rostral and caudal paraxial domains is a region that lacks *fgf8* expression (Figure 3K), which is required for presomitic mesodermal cells to segment into somites (Dubrulle et al., 2001). In 10-somite stage *pug* mutant embryos, *fgf8* expression appears normal in the somitic segments; however, the tail bud presomitic mesoderm domain is enlarged and the region that normally lacks *fgf8* expression is greatly reduced (Figures 3K and 3L). Expression of *paraxial protocadherin* (*papc*) also reveals that while segmentation appears normal, the unsegmented paraxial mesoderm is reduced in *pug* mutant embryos (Figures 3M and 3N). The tail bud domain of *papc* expression is also reduced, in contrast to the expanded tail bud domain of *fgf8*. This may reflect a change in cell fate within the tail bud that leads to a failure of cells to enter a tail differentiation program.

The apparent late role for *pug* in maintenance of the MHB and tail formation contrasts all other mutants described here, which display much earlier roles in the "zygotic" phase of development. Localization of a maternal mRNA to the discreet embryonic regions affected in *pug* mutants is not expected. Thus, we predict that the *pug* gene product is widely distributed, but required or activated by other localized factors. Both FGF and Wnt signaling pathways function in MHB maintenance (reviewed in Joyner et al., 2000; McMahon and Bradley, 1990), posterior tissue development (reviewed in Saga and Takeda, 2001; Yoshikawa et al., 1997), and limb development (reviewed in Capdevila and Izpisua Belmonte, 2001; Niswander, 2002), making these pathways

(F–K) Defective morphogenesis in late gastrula *pwg* embryos detected by *hgg1*, *pax2.1*, and *dlx3* expression. In wild-type embryos, *hgg1*$^+$ cells of the anterior mesendoderm have migrated past the anterior edge of the neural plate and underlie the *dlx3*+ nonneural ectoderm (F and I). The MHB and midline express *pax2.1* and *shh,* respectively. In mutant *pwg* embryos, *hgg1*$^+$ cells remain completely under the anterior neural plate between the *pax2.1* positive MHB and the nonneural ectoderm (G, H, J, and K). In approximately 30% of embryos, the anterior midline plunges into the yolk and *hgg1*$^+$ cells lie deep within the yolk instead of remaining on the yolk surface (arrowhead, [K]).

(L and M) At the 6-somite stage, anterior *shh*$^+$ cells also lie within the yolk (arrowhead). Paternal-effect mutant *cronos* (*crn*) (N–Q). (N) Wild-type embryo 1 dpf. (O) *crn* mutant embryo displays extensive neural necrosis (arrowhead). Terminal transferase assay of wild-type (P) and *crn* mutant (Q) embryos at 1 dpf.

(A–C, N–Q) Lateral view rostral to the left. (F–H) Dorso-anterior view anterior to the top. (I–M) Lateral view, dorsal to the right, animal to the top.

candidates for those defective in the *pug* mutant. Alternatively, *pug* may act more generally to initiate zygotic control of development, possibly via gene expression initiation or other regulatory mechanisms, and in this manner affect multiple tissues and possibly multiple pathways.

Other Body Plan Mutants

Two mutants displayed defects in the organization of the body plan, which may reflect a primary defect in morphogenesis or differentiation, rather than pattern formation. *blistered* (*bsd*) mutant embryos exhibit a dilated ventral tail vein with variable penetrance ($\sim$40%, Figures 4A and 4B). The affected embryos typically recover by 2 dpf and survive to adulthood. This phenotype may represent a defect in the structural integrity of the vessel or a subtle patterning defect. The phenotype is similar to but weaker than the edema observed in ventralized mutants of the BMP antagonists, *chordino* and *ogon* (Hammerschmidt et al., 1996; Solnica-Krezel et al., 1996), as well as *twisted gastrulation* depleted embryos (Ross et al., 2001), raising the possibility that this mutant is defective in the regulation of BMP signaling. However, we found no evidence for a reduction of any cell type expected from a change in dorsoventral patterning (data not shown).

The *pollywog* (*pwg*) mutant displays a dramatic change in body morphology without an obvious defect in pattern formation. At 1 dpf, *pwg* mutant embryos display a highly penetrant ($>$75%) failure to elevate their heads off the yolk, as well as widely spaced eyes on the yolk surface and a misshapen yolk ball and tube (Figures 4C–4E). Analysis of markers of ectodermal or mesodermal fates during gastrulation failed to reveal defects in embryonic pattern; however, marked defects in morphogenesis were observed (Figures 4F–4K). The anterior-posterior (AP) axis fails to extend fully and cells of the anterior midline are deflected laterally either leftward or rightward and occasionally plunge into the yolk (Figures 4F–4K). As neurulation proceeds, the phenotype becomes more pronounced. Analysis of *shh* expression in the midline at $\sim$6 somites indicates a shortening of the AP axis and extension of the anterior midline laterally and/or deep into the yolk instead of rostrally (Figures 4L and 4M and data not shown).

The anteriorward movement of the prechordal plate, the anterior midline mesoderm affected in *pollywog* mutants, is a basic morphogenetic process in vertebrates. The deflection of the prechordal plate cells may be caused by a lack of movement of the prechordal plate combined with normal rostral movement of the notochord, causing the prechordal tissue to buckle and laterally deflect or extend into the yolk. Our results suggest that the anterior prechordal plate cells migrate independently of the posterior midline and in *pollywog* mutants do not receive the proper directional signals that instruct their migration path.

Paternal-Effect Mutants

We identified five paternal-effect mutants. Although we expected to find male sterile mutants (Dosch et al., 2004), we were surprised to identify five paternal-effect mutants. For these mutants, the male parent was the sole cause of the embryonic defect, not the female. The paternal-effect mutants display a pleiotropic degeneration phenotype associated with widespread cell death (Figures 4N–4Q), similar to the large class of maternal-effect degeneration mutants. In three of the four mutants kept of this class, the cell death phenotype was combined with a low fertilization rate (5%–10% fertilized for *p5bn*, *p95re*, and *cronos* [*crn*]).

The paternal-effect mutants reveal a crucial contribution of the sperm to embryonic development in the zebrafish. We screened about 500 paternal genomes compared to 600 maternal genomes, and identified five paternal-effect and 63 maternal-effect mutants (five potential female sterile mutants excluded), respectively. Although the major contribution to embryonic development comes from the mother, the frequency of paternal-effect mutations shows a larger role than we expected for the sperm. The sperm contributes a haploid genome and the only centrosome in the embryo. Unlike mammals, there is no evidence of imprinting in zebrafish, so the phenotype must result from another defect associated with the male contribution. In *Drosophila*, three of four identified paternal-effect mutants exhibit meiotic or early mitotic defects causing embryonic aneuploidy (reviewed in Fitch et al., 1998). Thus some of our paternal-effect phenotypes may be caused by similar defects associated with the composition of the paternal chromatin or centrosome.

Adult Phenotypes

In raising F3 fish to adulthood, we observed numerous recessive, morphologically visible adult mutant phenotypes. We kept a subset of these and successfully recovered 17 of 18 mutants tested. These mutants display defective blood homeostasis (one mutant), altered adult pigmentation (eight mutants), altered body shape (five), large eyes (one), gill and fin defects (one), or an enlarged heart (one) (examples in Supplemental Data). The *pink panther* (*pkp*) mutant displays an irregular pigmentation pattern including an absence of stripes in the fins and interrupted body stripes. The *cut throat* (*ctr*) mutant exhibits exposed gills due to small or crumpled opercula, as well as crumpled fins. The blood homeostasis mutant *leopold* (*lpd*) bleeds profusely around the fins and mouth after normal handling. The *p26ac* mutant displays a large ventral protrusion below the pectoral fins, which dissection reveals is an enlarged heart. The *p71fmc* mutant displays a short, twisted body, and almost complete loss of the tail, with the exception of a relatively normal tail fin. The ability to identify viable adult phenotypes in a systematic screen presents an opportunity to develop zebrafish models for childhood and adult human genetic diseases.

Conclusion

In a maternal-effect mutant screen of 600 mutagenized genomes in the zebrafish, we identified a large fraction of mutants that first manifested their phenotypes at or following the onset of zygotic transcription. Some of these mutant genes likely function prior to the onset of zygotic transcription and may exhibit an earlier morphological or molecular phenotype that we have not yet identified. However, for many of the mutants, the first requirement

for the maternal gene product will be at or after the onset of zygotic transcription, reflecting a persistence of maternal influence on the later "zygotic" period of embryogenesis.

Our screen was designed to identify genes that function both maternally and zygotically in the same process and require loss of both components to exhibit an embryonic phenotype. However, we identified no recessive maternal-zygotic mutants in approximately 300 genomes screened. The absence of this class of mutants may reflect an essential zygotic function for most maternally and zygotically expressed genes, precluding the survival of homozygous mutant individuals to adulthood. Some of our maternal-effect mutants may also be hypomorphic alleles of maternal-zygotic genes that are sufficient zygotically, but not maternally. There is precedence for such mutant alleles from the fly (Gerttula et al., 1988; Perrimon et al., 1986). However, in such cases, we would expect an increased penetrance or severity of the phenotype in homozygous mutant embryos derived from homozygous females. So far we have not detected such zygotic enhancement of a maternal phenotype; however, all of the mutants have not been rigorously tested.

The diverse range of phenotypes recovered and the absence of expected classes of mutants, such as those defective in germ layer induction, indicate that more maternal-effect genes and maternally controlled processes remain to be identified in future screens. The unique features of the mutants that we did recover demonstrate that a four-generation maternal-effect screen is a powerful tool for identifying mutants that can be used to dissect the molecular control of early vertebrate development.

Experimental Procedures

Fish Mutagenesis

Mutagenesis and screening strategy are presented in the companion article in this issue (Dosch et al., 2004).

Whole-Mount In Situ Hybridization

We carried out whole-mount in situ hybridization essentially as described (Schulte-Merker et al., 1992). In situ probes were *chordin* (Miller-Bertoglio et al., 1997), *no tail* (Schulte-Merker et al., 1992), *pax2.1* (Krauss et al., 1992), *goosecoid* (Schulte-Merker et al., 1994), *fgf8* (Furthauer et al., 1997), *sonic hedgehog* (Krauss et al., 1993), *bmp2b* (Nikaido et al., 1997), *eve1* (Joly et al., 1993), *spadetail* (Griffin et al., 1998), *dharma* (Yamanaka et al., 1998), *tbx6* (Hug et al., 1997), *hgg1* (Thisse et al., 1994), *papc* (Yamamoto et al., 1998), and *dlx3* (Akimenko et al., 1994).

Photography

Images were captured on Prog/Res/3012 (Kontron Elektronic) and Cool Snap and Cool Snap *cf* using Openlab (Improvision), IPlab (Scanalytics), iVision (DVL Software), and Adobe Photoshop (Adobe Systems) software. Images were processed in Abobe Photoshop and Adobe Illustrator.

Time-Lapse Video

Embryos from natural matings were collected within a 15 min time window. For analysis of *screeching halt*, mutant and wild-type embryos in their chorions were mounted in E3 medium in wells cut into electrical tape. For epiboly mutants, the embryos were dechorionated, oriented, and mounted at sphere stage in 0.12% agarose (Type IV: low gelling temperature, Sigma) in embryo media supplemented with 10 mM HEPES (pH 7.2). Images were captured on a Zeiss Axioplan2 microscope fitted with a Marzhauser X-Y motorized stage and a Cool Snap camera. Microscope, stage, and image acquisition were controlled using Openlab software (Improvision). Individual images within a time series were measured for animal-vegetal length and the distance from the animal pole to the margin. Measurements for each series of images were performed sequentially three times to correct for measurement error.

Acknowledgments

We thank past and present fish facility staff, including D. Cobb, D. Peterson, W. Vought, W. Kilgore, D. Degefa, C. Miller, and H. Robinson-Bey. We thank M. Bartolomei, S. DiNardo, M. Granato, and F. Marlow for valuable comments on the manuscript. K.A.M. coauthored this article in his private capacity. The views expressed in the article do not necessarily represent the views of the NIH, the DHHS, or the United States. This work was supported in part by research Grant No. 1-FY02-24 from the March of Dimes Birth Defects Foundation, an NIH grant (ES11248), and an award from the American Heart Association to M.C.M., DAAD-fellowship (Deutscher Akademischer Austauschdienst) to R.D., NRSA fellowship (F32-GM019803) to D.S.W., American Cancer Society fellowship (PF-98-037-01) to K.A.M., and NIH training program grant HD07516 to A.P.W.

Received: July 26, 2003
Revised: March 29, 2004
Accepted: March 29, 2004
Published: June 7, 2004

References

Abdelilah, S., Mountcastle-Shah, E., Harvey, M., Solnica-Krezel, L., Schier, A.F., Stemple, D.L., Malicki, J., Neuhauss, S.C., Zwartkruis, F., Stainier, D.Y., et al. (1996). Mutations affecting neural survival in the zebrafish *Danio rerio*. Development *123*, 217–227.

Akimenko, M.A., Ekker, M., Wegner, J., Lin, W., and Westerfield, M. (1994). Combinatorial expression of three zebrafish genes related to distal-less: part of a homeobox gene code for the head. J. Neurosci. *14*, 3475–3486.

Andeol, Y. (1994). Early transcription in different animal species: implications for transition from maternal to zygotic control of development. Roux's Archive of Dev. Biol. *204*, 3–10.

Bachvarova, R., and De Leon, V. (1980). Polyadenylated RNA of mouse ova and loss of maternal RNA in early development. Dev. Biol. *74*, 1–8.

Bachvarova, R., and Moy, K. (1985). Autoradiographic studies on the distribution of labeled maternal RNA in early mouse embryos. J. Exp. Zool. *233*, 397–403.

Betchaku, T., and Trinkaus, J.P. (1978). Contact relations, surface activity, and cortical microfilaments of marginal cells of the enveloping layer and of the yolk syncytial and yolk cytoplasmic layers of Fundulus before and during epiboly. J. Exp. Zool. *206*, 381–426.

Bolton, V.N., Oades, P.J., and Johnson, M.H. (1984). The relationship between cleavage, DNA replication, and gene expression in the mouse 2-cell embryo. J. Embryol. Exp. Morphol. *79*, 139–163.

Bourc'his, D., Xu, G.L., Lin, C.S., Bollman, B., and Bestor, T.H. (2001). Dnmt3L and the establishment of maternal genomic imprints. Science *294*, 2536–2539.

Capdevila, J., and Izpisua Belmonte, J.C. (2001). Patterning mechanisms controlling vertebrate limb development. Annu. Rev. Cell Dev. Biol. *17*, 87–132.

Christians, E., Davis, A.A., Thomas, S.D., and Benjamin, I.J. (2000). Maternal effect of Hsf1 on reproductive success. Nature *407*, 693–694.

Dosch, R., Wagner, D.S., Mintzer, K.A., Runke, G., Wiemelt, A.P., and Mullins, M.C. (2004). Maternal control of vertebrate development before the midblastula transition: mutants from the zebrafish I. Dev. Cell *6*, this issue, 771–780.

Dubrulle, J., McGrew, M.J., and Pourquie, O. (2001). FGF signaling controls somite boundary position and regulates segmentation

clock control of spatiotemporal Hox gene activation. Cell *106*, 219–232.

Fitch, K.R., Yasuda, G.K., Owens, K.N., and Wakimoto, B.T. (1998). Paternal effects in *Drosophila*: implications for mechanisms of early development. Curr. Top. Dev. Biol. *38*, 1–34.

Flach, G., Johnson, M.H., Braude, P.R., Taylor, R.A., and Bolton, V.N. (1982). The transition from maternal to embryonic control in the 2-cell mouse embryo. EMBO J. *1*, 681–686.

Fogarty, P., Campbell, S.D., Abu-Shumays, R., Phalle, B.S., Yu, K.R., Uy, G.L., Goldberg, M.L., and Sullivan, W. (1997). The *Drosophila* grapes gene is related to checkpoint gene chk1/rad27 and is required for late syncytial division fidelity. Curr. Biol. *7*, 418–426.

Furthauer, M., Thisse, C., and Thisse, B. (1997). A role for FGF-8 in the dorsoventral patterning of the zebrafish gastrula. Development *124*, 4253–4264.

Furutani-Seiki, M., Jiang, Y.J., Brand, M., Heisenberg, C.P., Houart, C., Beuchle, D., van Eeden, F.J., Granato, M., Haffter, P., Hammerschmidt, M., et al. (1996). Neural degeneration mutants in the zebrafish, *Danio rerio*. Development *123*, 229–239.

Gans, M., Audit, C., and Masson, M. (1975). Isolation and characterization of sex-linked female-sterile mutants in *Drosophila melanogaster*. Genetics *81*, 683–704.

Gerttula, S., Jin, Y.S., and Anderson, K.V. (1988). Zygotic expression and activity of the *Drosophila* Toll gene, a gene required maternally for embryonic dorsal-ventral pattern formation. Genetics *119*, 123–133.

Golling, G., Amsterdam, A., Sun, Z., Antonelli, M., Maldonado, E., Chen, W., Burgess, S., Haldi, M., Artzt, K., Farrington, S., et al. (2002). Insertional mutagenesis in zebrafish rapidly identifies genes essential for early vertebrate development. Nat. Genet. *31*, 135–140.

Griffin, K.J., Amacher, S.L., Kimmel, C.B., and Kimelman, D. (1998). Molecular identification of *spadetail*: regulation of zebrafish trunk and tail mesoderm formation by T-box genes. Development *125*, 3379–3388.

Gritsman, K., Zhang, J., Cheng, S., Heckscher, E., Talbot, W.S., and Schier, A.F. (1999). The EGF-CFC protein *one-eyed pinhead* is essential for nodal signaling. Cell *97*, 121–132.

Hammerschmidt, M., Pelegri, F., Mullins, M.C., Kane, D.A., van Eeden, F.J., Granato, M., Brand, M., Furutani-Seiki, M., Haffter, P., Heisenberg, C.P., et al. (1996). *dino* and *mercedes*, two genes regulating dorsal development in the zebrafish embryo. Development *123*, 95–102.

Hibi, M., Hirano, T., and Dawid, I.B. (2002). Organizer formation and function. In Pattern Formation in Zebrafish, L. Solnica-Krezel, ed. (New York, Springer-Verlag), pp. 48–71.

Howell, C.Y., Bestor, T.H., Ding, F., Latham, K.E., Mertineit, C., Trasler, J.M., and Chaillet, J.R. (2001). Genomic imprinting disrupted by a maternal effect mutation in the *Dnmt1* gene. Cell *104*, 829–838.

Hug, B., Walter, V., and Grunwald, D.J. (1997). *tbx6*, a Brachyury-related gene expressed by ventral mesendodermal precursors in the zebrafish embryo. Dev. Biol. *183*, 61–73.

Ikegami, R., Hunter, P., and Yager, T.D. (1999). Developmental activation of the capability to undergo checkpoint-induced apoptosis in the early zebrafish embryo. Dev. Biol. *209*, 409–433.

Joly, J.S., Joly, C., Schulte-Merker, S., Boulekbache, H., and Condamine, H. (1993). The ventral and posterior expression of the zebrafish homeobox gene *eve1* is perturbed in dorsalized and mutant embryos. Development *119*, 1261–1275.

Joyner, A.L., Liu, A., and Millet, S. (2000). Otx2, Gbx2 and Fgf8 interact to position and maintain a mid-hindbrain organizer. Curr. Opin. Cell Biol. *12*, 736–741.

Kane, D.A., and Kimmel, C.B. (1993). The zebrafish midblastula transition. Development *119*, 447–456.

Kane, D.A., Hammerschmidt, M., Mullins, M.C., Maischein, H.M., Brand, M., van Eeden, F.J., Furutani-Seiki, M., Granato, M., Haffter, P., Heisenberg, C.P., et al. (1996). The zebrafish epiboly mutants. Development *123*, 47–55.

Kelly, C., Chin, A.J., Leatherman, J.L., Kozlowski, D.J., and Weinberg, E.S. (2000). Maternally controlled β-catenin-mediated signaling is required for organizer formation in the zebrafish. Development *127*, 3899–3911.

Krauss, S., Johansen, T., Korzh, V., and Fjose, A. (1991). Expression of the zebrafish paired box gene pax[zf-b] during early neurogenesis. Development *113*, 1193–1206.

Krauss, S., Maden, M., Holder, N., and Wilson, S.W. (1992). Zebrafish pax[b] is involved in the formation of the midbrain-hindbrain boundary. Nature *360*, 87–89.

Krauss, S., Concordet, J.P., and Ingham, P.W. (1993). A functionally conserved homolog of the *Drosophila* segment polarity gene hh is expressed in tissues with polarizing activity in zebrafish embryos. Cell *75*, 1431–1444.

Leader, B., Lim, H., Carabatsos, M.J., Harrington, A., Ecsedy, J., Pellman, D., Maas, R., and Leder, P. (2002). Formin-2, polyploidy, hypofertility and positioning of the meiotic spindle in mouse oocytes. Nat. Cell Biol. *4*, 921–928.

McMahon, A.P., and Bradley, A. (1990). The Wnt-1 (int-1) proto-oncogene is required for development of a large region of the mouse brain. Cell *62*, 1073–1085.

Miller-Bertoglio, V.E., Fisher, S., Sanchez, A., Mullins, M.C., and Halpern, M.E. (1997). Differential regulation of chordin expression domains in mutant zebrafish. Dev. Biol. *192*, 537–550.

Miller-Bertoglio, V., Carmany-Rampey, A., Furthauer, M., Gonzalez, E.M., Thisse, C., Thisse, B., Halpern, M.E., and Solnica-Krezel, L. (1999). Maternal and zygotic activity of the zebrafish *ogon* locus antagonizes BMP signaling. Dev. Biol. *214*, 72–86.

Mintzer, K.A., Lee, M.A., Runke, G., Trout, J., Whitman, M., and Mullins, M.C. (2001). *lost-a-fin* encodes a type I BMP receptor, Alk8, acting maternally and zygotically in dorsoventral pattern formation. Development *128*, 859–869.

Mullins, M.C., Hammerschmidt, M., Haffter, P., and Nüsslein-Volhard, C. (1994). Large-scale mutagenesis in the zebrafish: in search of genes controlling development in a vertebrate. Curr. Biol. *4*, 189–202.

Newport, J., and Kirschner, M. (1982a). A major developmental transition in early *Xenopus* embryos: I. Characterization and timing of cellular changes at the midblastula stage. Cell *30*, 675–686.

Newport, J., and Kirschner, M. (1982b). A major developmental transition in early *Xenopus* embryos: II. Control of the onset of transcription. Cell *30*, 687–696.

Nikaido, M., Tada, M., Saji, T., and Ueno, N. (1997). Conservation of BMP signaling in zebrafish mesoderm patterning. Mech. Dev. *61*, 75–88.

Niswander, L. (2002). Interplay between the molecular signals that control vertebrate limb development. Int. J. Dev. Biol. *46*, 877–881.

Perrimon, N., Mohler, D., Engstrom, L., and Mahowald, A.P. (1986). X-linked female-sterile loci in *Drosophila melanogaster*. Genetics *113*, 695–712.

Raftery, L.A., Twombly, V., Wharton, K., and Gelbart, W.M. (1995). Genetic screens to identify elements of the decapentaplegic signaling pathway in *Drosophila*. Genetics *139*, 241–254.

Renard, J.P., Baldacci, P., Richoux-Duranthon, V., Pournin, S., and Babinet, C. (1994). A maternal factor affecting mouse blastocyst formation. Development *120*, 797–802.

Ross, J.J., Shimmi, O., Vilmos, P., Petryk, A., Kim, H., Gaudenz, K., Hermanson, S., Ekker, S.C., O'Connor, M.B., and Marsh, J.L. (2001). Twisted gastrulation is a conserved extracellular BMP antagonist. Nature *410*, 479–483.

Saga, Y., and Takeda, H. (2001). The making of the somite: molecular events in vertebrate segmentation. Nat. Rev. Genet. *2*, 835–845.

Schulte-Merker, S., Ho, R.K., Herrmann, B.G., and Nüsslein-Volhard, C. (1992). The protein product of the zebrafish homologue of the mouse T gene is expressed in nuclei of the germ ring and the notochord of the early embryo. Development *116*, 1021–1032.

Schulte-Merker, S., Hammerschmidt, M., Beuchle, D., Cho, K.W., De Robertis, E.M., and Nüsslein-Volhard, C. (1994). Expression of

zebrafish *goosecoid* and *no tail* gene products in wild-type and mutant no tail embryos. Development *120*, 843–852.

Schupbach, T., and Wieschaus, E. (1989). Female sterile mutations on the second chromosome of *Drosophila melanogaster*. I. Maternal effect mutations. Genetics *121*, 101–117.

Sekelsky, J.J., Newfeld, S.J., Raftery, L.A., Chartoff, E.H., and Gelbart, W.M. (1995). Genetic characterization and cloning of *mothers against dpp*, a gene required for decapentaplegic function in *Drosophila melanogaster*. Genetics *139*, 1347–1358.

Shimuta, K., Nakajo, N., Uto, K., Hayano, Y., Okazaki, K., and Sagata, N. (2002). Chk1 is activated transiently and targets Cdc25A for degradation at the *Xenopus* midblastula transition. EMBO J. *21*, 3694–3703.

Sibon, O.C., Stevenson, V.A., and Theurkauf, W.E. (1997). DNA-replication checkpoint control at the *Drosophila* midblastula transition. Nature *388*, 93–97.

Sibon, O.C., Laurencon, A., Hawley, R., and Theurkauf, W.E. (1999). The *Drosophila* ATM homologue Mei-41 has an essential checkpoint function at the midblastula transition. Curr. Biol. *9*, 302–312.

Sokol, S.Y. (1999). Wnt signaling and dorso-ventral axis specification in vertebrates. Curr. Opin. Genet. Dev. *9*, 405–410.

Solnica-Krezel, L., and Driever, W. (1994). Microtubule arrays of the zebrafish yolk cell: organization and function during epiboly. Development *120*, 2443–2455.

Solnica-Krezel, L., Stemple, D.L., Mountcastle-Shah, E., Rangini, Z., Neuhauss, S.C., Malicki, J., Schier, A.F., Stainier, D.Y., Zwartkruis, F., Abdelilah, S., and Driever, W. (1996). Mutations affecting cell fates and cellular rearrangements during gastrulation in zebrafish. Development *123*, 67–80.

Steward, R., McNally, F.J., and Schedl, P. (1984). Isolation of the dorsal locus of *Drosophila*. Nature *311*, 262–265.

Strahle, U., and Jesuthasan, S. (1993). Ultraviolet irradiation impairs epiboly in zebrafish embryos: evidence for a microtubule-dependent mechanism of epiboly. Development *119*, 909–919.

Terracol, R., and Lengyel, J.A. (1994). The thick veins gene of *Drosophila* is required for dorsoventral polarity of the embryo. Genetics *138*, 165–178.

Thisse, C., Thisse, B., Halpern, M.E., and Postlethwait, J.H. (1994). Goosecoid expression in neurectoderm and mesendoderm is disrupted in zebrafish cyclops gastrulas. Dev. Biol. *164*, 420–429.

Tong, Z.B., Gold, L., Pfeifer, K.E., Dorward, H., Lee, E., Bondy, C.A., Dean, J., and Nelson, L.M. (2000). Mater, a maternal effect gene required for early embryonic development in mice. Nat. Genet. *26*, 267–268.

Warga, R.M., and Kimmel, C.B. (1990). Cell movements during epiboly and gastrulation in zebrafish. Development *108*, 569–580.

Wu, X., Viveiros, M.M., Eppig, J.J., Bai, Y., Fitzpatrick, S.L., and Matzuk, M.M. (2003). Zygote arrest 1 (*Zar1*) is a novel maternal-effect gene critical for the oocyte-to-embryo transition. Nat. Genet. *33*, 187–191.

Yamamoto, A., Amacher, S.L., Kim, S.H., Geissert, D., Kimmel, C.B., and De Robertis, E.M. (1998). Zebrafish paraxial protocadherin is a downstream target of spadetail involved in morphogenesis of gastrula mesoderm. Development *125*, 3389–3397.

Yamanaka, Y., Mizuno, T., Sasai, Y., Kishi, M., Takeda, H., Kim, C.H., Hibi, M., and Hirano, T. (1998). A novel homeobox gene, *dharma*, can induce the organizer in a non-cell-autonomous manner. Genes Dev. *12*, 2345–2353.

Yoshikawa, Y., Fujimori, T., McMahon, A.P., and Takada, S. (1997). Evidence that absence of Wnt-3a signaling promotes neuralization instead of paraxial mesoderm development in the mouse. Dev. Biol. *183*, 234–242.

Zalokar, M., Audit, C., and Erk, I. (1975). Developmental defects of female-sterile mutants of *Drosophila melanogaster*. Dev. Biol. *47*, 419–432.